Desalination and Water Treatment
www.deswater.com

doi: 10.5004/dwt.2021.27142

225 (2021) 402–412
June

Treatment of landfill leachate from Fez City by combined Fenton and adsorption processes using Moroccan bentonite clay

Imane El Mrabet[a,*], Mourad Benzina[b], Hicham Zaitan[a,*]

[a]*Processes, Materials and Environment Laboratory (LPME), Department of Chemistry, Faculty of Sciences and Technology of Fez, Sidi Mohamed Ben Abdellah University, B.P. 2202, Fez, Morocco, emails: imane.elmrabet@usmba.ac.ma (I. El Mrabet), hicham.zaitan@usmba.ac.ma (H. Zaitan)*
[b]*Laboratory of Water Energy Environment, National School of Engineers of Sfax, University of Sfax, Sfax, Tunisia, email: mourad.benzina@enis.rnu.tn*

Received 24 December 2019; Accepted 4 January 2021

ABSTRACT

This work deals with the study of the feasibility of landfill leachate treatment (Fez city, Morocco), using sequential processes combining Fenton and adsorption onto natural local bentonite clay. Thus, the operational conditions of the Fenton process were firstly optimized with 2,000 mg L^{-1} of Fe^{2+} and 2,500 mg L^{-1} of H_2O_2 at pH = 3, which removed 73% of the chemical oxygen demand (COD) and 92% of the color from the raw leachate. Then, raw Moroccan bentonite was characterized by nitrogen adsorption–desorption, scanning electron microscopy-energy dispersive X-ray analysis, X-ray diffraction, and Fourier transforms infrared spectroscopy. The results indicate that the bentonite is characterized by a heterogeneous surface with irregular particle sizes and the presence of the montmorillonite as the major component. The bentonite presented characteristics of mesoporous material with Brunauer–Emmet–Teller (BET) surface area and total volume of pores of 51.7 m^2 g^{-1} and 0.11 cm^3 g^{-1}, respectively. The natural bentonite clay was used as an adsorbent for the pretreated leachate (PL). The effect of adsorbent dosage, effluent pH, contact time, and temperature on the adsorption efficiency was investigated. Pseudo-second-order and Freundlich were the most suitable models to fit the experimental kinetic and the isotherm data of the adsorption, respectively. Therefore, 73% of COD and 96.5% of color removal were observed in Fenton treatment alone. The application of the Fenton process (2,500 mg L^{-1} of H_2O_2, 2,000 mg L^{-1} of Fe^{2+}, pH 3, and 1 h of contact time) coupled with adsorption (3 g L^{-1} of bentonite dosage, pH 5 and 5 h of contact time, and T = 35°C) has achieved a total COD and color removal of 84% and 98%, respectively. This indicates that the combination process that involves Fenton followed by the adsorption process onto natural bentonite adsorbent would be an ideal option for leachate treatment.

Keywords: Landfill leachate; Fenton; Adsorption; Natural bentonite; COD

1. Introduction

In Morocco, only 10% of solid wastes are recycled, though, the large part is mainly managed by municipal landfills. However, leachate resulting from this management way presents major secondary pollution, because of its high and complex pollutants load. Therefore, the huge amounts of leachate present an extreme contamination risk for soil, groundwater, and surface water. Thus, the treatment of this leachate is highly required before discharging it into the environment.

Indeed, there has been a growing interest in developing various methods, single or combined, for leachate contaminants elimination according to its age and

* Corresponding authors.

composition [1–5]. For instance, Azmi et al. [6] used sugarcane bagasse activated carbon as an adsorbent to reduce 83.61% of COD from anaerobic stabilized landfill leachate. A study by Assou et al. [7] indicated that the coagulation–flocculation process by $FeCl_3$ and $Al_2(SO_4)_3$ reached 67% and 60%, respectively, in terms of the COD yields. Anoxic aged refuse-based bioreactor (ARB) for biological leachate pretreatment studied by Hassan et al. [8] allowed a COD removal of 72%. Li et al. [9] assessed the treatment of landfill leachate which achieved 85% COD removal using electrocoagulation. The chemical oxidation by $S_2O_8^{2-}$/Fe^{2+}/UV-A removed 70% of COD from stabilized landfill leachate. Cherni et al. [11] noted that the application of the photocatalytic process with TiO_2/Ag nanocomposite to removes 70% of COD from Tunisian landfill leachate.

Moreover, many other studies reported a high performance of the Fenton process for leachate treatment, as one of the advanced oxidation processes (AOPs). Hence, the treatment by Fenton process removed the majority of the COD from leachate of different countries landfills: 69% (Tehran, Iran) [12], 55.91% (Golestan, Iran) [13], 85% (Ganzhou Refuse Landfill, Jiangxi Province of China) [14], 75% (Barcelona, Spain) [15], 80% (Slovenia) [16], 70% (Florida, USA) [17], and 54%–98% (Istanbul, Turkey) [1]. Nevertheless, the significant values in terms of COD percentage removal obtained by the single Fenton process do not necessarily mean that the reached COD value meets the strict standards for direct discharging of the liquids into the environment. Therefore, applying the adsorption process is generally suggested as a secondary treatment step to remove the residual contaminants.

In this sense, the use of natural adsorbents is becoming increasingly relevant for contaminants removal from wastewater due to their high availability, sustainability, and eco-friendly efficiency [18–20]. Among these, bentonite clay is considered one of the most efficient adsorbents widely assessed by review bibliography in its raw or modified form used in wastewater treatment [21–24]. This clay provided excellent adsorption capacities for pollutants' removal from real and synthetic liquid effluents [25–29]. According to Derakhshani et al. [26], the commercial nanoparticles of bentonite were successfully used to remove humic acid reaching the adsorption capacity of 21.58 mg g^{-1}. The retention of bisphenol A from landfill leachate was studied by Li et al. [28] using raw commercial bentonite that achieved an adsorption capacity of 3.41 mg g^{-1}, while the modification of the same bentonite with cationic surfactant hexadecyl trimethyl ammonium bromide (HTAB) enhanced the retention capacity 10.45 mg g^{-1}. Hajjaji et al. [30] reported that the adsorption capacities of MB and Zn ions by raw bentonite were about 2.2 and 1.1 mmol g^{-1} of natural bentonite, while the acid-activation of the bentonite reduced the maximum uptake of MB and Zn ions by 30% and 95%. Huang et al. [31] synthesized organobentonite to enhance the removal of dyes, where the maximum adsorption capacity was noticed at 173.5 and 157.4 mg g^{-1} for Rhodamine B and Acid red 1, respectively. Natural bentonite clay modified with calcium had a great efficiency for metal ions removal from wastewaters, which removed 73% of Cd(II) and 100% of Pb(II) as described by Meneguin et al. [32]. The synthesis of Fe_3O_4/Bentonite nanocomposite was investigated by Khatamian et al. [23] and reached a great potential for the removal of nitrate (79%) BOD (84.88%) and COD (88.8%) from the industrial wastewater.

In the same context, the current work aims to investigate the potentiality of Moroccan raw bentonite as a natural adsorbent for the enhancement of COD removal from pretreated leachate (PL) (Fez landfill, Morocco) by the Fenton process, and which optimal parameters were already determined in our previous work [33]. Thus, the characterization of raw bentonite was conducted using X-ray diffraction (XRD), Fourier transform infrared (FTIR), scanning electron microscopy (SEM) coupled to energy-dispersive X-ray spectroscopy (SEM-EDX), and N_2 adsorption–desorption. Afterwards, the main parameters affecting the adsorption process were optimized, mainly: adsorbent mass, initial pH leachate, time contact, and temperature, in terms of COD removal from the PL sample.

2. Experimental

2.1. Chemicals and materials

The chemicals used in the experiments of this study for leachate treatment were all recognized analytical reagents grade and supplied by Sigma-Aldrich Chimie S.a.r.l. (Lyon, France): ferrous sulfate ($FeSO_4{\cdot}7H_2O$); hydrogen peroxide (H_2O_2, 30% (w/w)); sulfuric acid (H_2SO_4); sodium hydroxide (NaOH).

The natural bentonite clay used for the adsorption step was provided from the northeastern Rif region of Morocco.

2.2. Leachate sampling

Landfill leachate samples were collected from Fez city urban sanitary landfill, northwestern Morocco (34°00′16.6″N 4°55′44.5″W) (Fig. 1). The collected leachate sample was stored into 25 L opaque plastic bottles at 4°C in order to minimize leachate decomposition caused by microbial activity.

2.3. Leachate characterization

The physicochemical characteristics of landfill leachate and the treatment by the Fenton process were described in our previous study [33]. The main parameters were measured according to the standard methods for the examination of water and wastewater [34]. Turbidity was determined using a turbid-meter "HI 88713 – ISO HANNA". Chlorides concentration was quantified by volumetric dosage using Mohr method. N-nitrate, N-nitrite, and sulfate were measured with the spectrophotometric method at 415, 435, and 650 nm, respectively. The measurement of COD was carried out using the spectrophotometric method based on the determination of potassium dichromate excess at 600 nm [35]. UV–visible absorption measurements were obtained using a UV2300 II spectrophotometer with 1 cm quartz cells. Inductively coupled plasma atomic emission spectroscopy analysis ICP-AES (Activa, Jobinyvon) was used to quantify the concentration of metals.

Due to the complex composition of landfill leachate, COD is considered as the major indicator of organic pollution in landfill leachate and is used to evaluate the efficiency

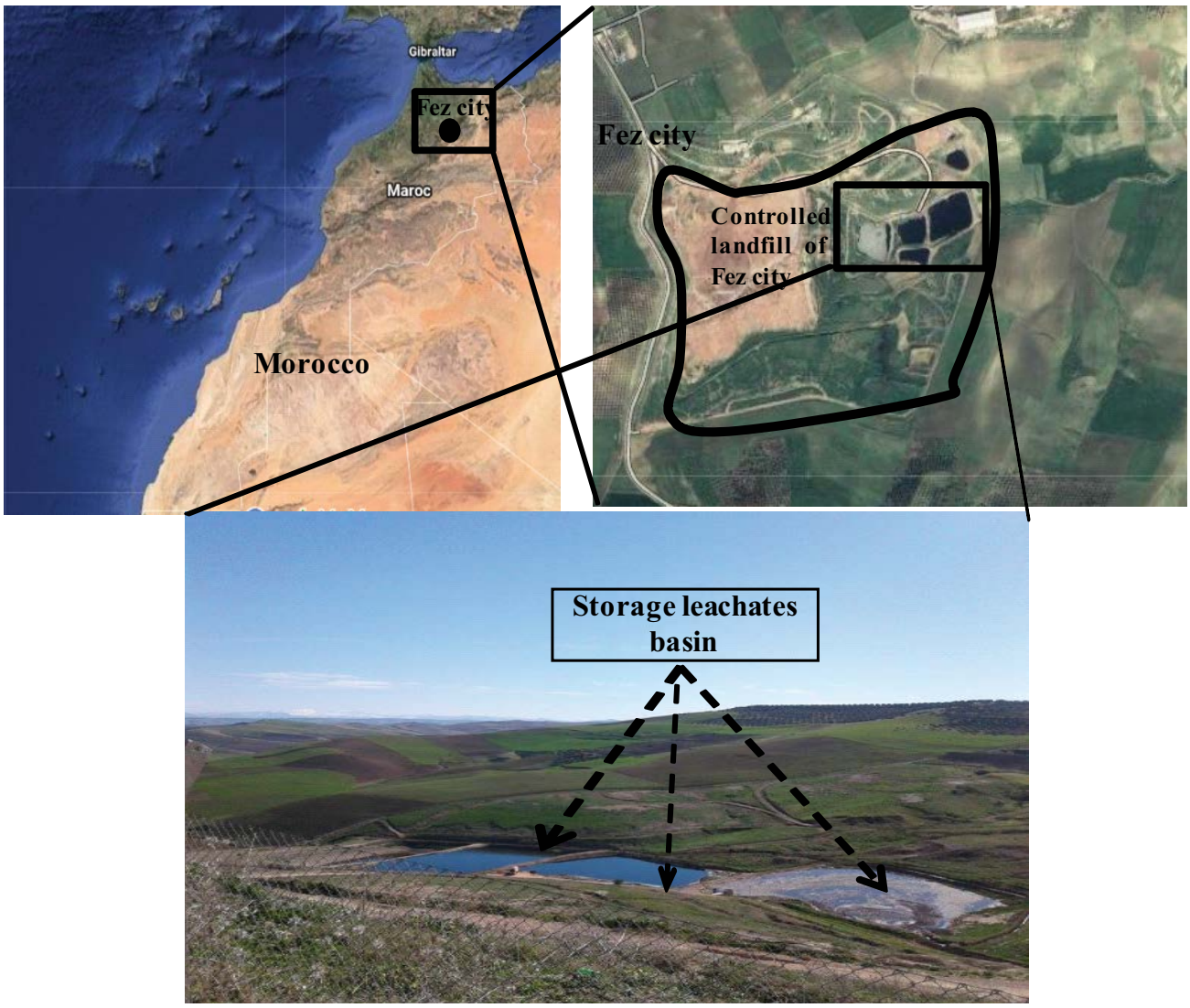

Fig. 1. Satellite image of the controlled landfill in Fez and photograph of the leachate storage basins at leachate.

of the applied treatment processes. Nothing also that some measurements required leachate sample dilutions.

2.4. Adsorbent preparation and characterization

The natural bentonite was firstly crushed, washed several times with distilled water, dried at 110°C for 24 h, and was finally ground into a powder (<20 μm) ready to use for the characterization and the adsorption tests.

The specific surface area and pore diameter of the adsorbent were measured with ASAP 2020 Micromeritics sorption analyzer (Norcross, GA, USA) based on N_2 adsorption/desorption at 77 K in a relative pressure range of P/P_0 = 0.06–0.3 and described by Brunauer–Emmett–Teller (BET) theory [36]. The total pore volume was determined from the adsorbed N_2 volume at P/P_0 = 0.9. Before the nitrogen sorption measurement, the bentonite sample was degassed at 120°C in a vacuum condition for 24 h.

Bentonite was characterized using a powder X-ray diffractometer (X'pert-PRO) with CuKα radiation (30 mA, 40 kV). The surface morphology and chemical composition of bentonite surface were investigated using SEM coupled with an energy dispersive X-ray analyzer (EDX) (Quanta 200).

The bentonite was also characterized by FTIR spectrophotometer (VERTEX 70) in a wavenumber range of 400–4,000 cm^{-1} for analyzing the functional groups present on the adsorbent surface.

2.5. Fenton process

Firstly, the raw leachate sample was pretreated using the optimal conditions obtained during our previous study [33]: 2,500 mg L^{-1} of H_2O_2, 2,000 mg L^{-1} of Fe^{2+}, pH = 3, and 1 h of contact time, following the experimental protocol reported in the same work.

The pretreated sample was finally neutralized at pH = 7 using 1 M NaOH. A stock solution was prepared (COD = 1,400 mg L^{-1}), denoted as PL, and preserved in an opaque flask at 4°C to be used for the adsorption tests.

2.6. Adsorption process

In order to evaluate the adsorbent mass effect, a fixed volume of this sample was poured into a series of opaque flasks and increasing amounts of bentonite were added. The mixture was stirred at 200 rpm at room temperature. Then, the samples were centrifuged in order to analyze the residual concentration of the COD and UV-visible spectrum.

The same procedure was followed to study the pH effect using a fixed adsorbent dosage and adjusted leachate pH values (2–12) using 1 M H_2SO_4 or 1 M NaOH solutions. Afterwards the kinetic of adsorption was investigated under the optimal conditions of mass bentonite and leachate pH. Finally, the temperature effect was studied at 3 levels (25°C, 30°C, and 35°C) in order to study the isotherm mechanism.

2.6.1. Evaluation of the bentonite performance

The COD removal in terms of percentage was obtained by the following equation:

$$\text{COD Removal}(\%) = \frac{\text{COD}_i - \text{COD}_{e,t}}{\text{COD}_i} \times 100 \quad (1)$$

The adsorbed amount of organic compounds of the leachate sample (mg g^{-1}) at equilibrium (q_e) and at a different time (q_t) was calculated using the following formula:

$$q_{e,t} = \frac{(\text{COD}_i - \text{COD}_{e,t})V}{m} \quad (2)$$

where COD_i is the initial COD value of PL and $\text{COD}_{e,t}$ at equilibrium and at a different moment of adsorption (mg L^{-1}), V is the sample leachate volume (L), and m is the bentonite mass (g).

2.6.2. Kinetic study

In order to examine the kinetic experimental data and to interpret the adsorption behavior, pseudo-first-order and pseudo-second-order kinetic models were applied and analyzed based on the regression coefficient (R^2).

The pseudo-first-order is given by the expression of Lagergren with the following equation [37]:

$$q_t = q_e\left(1 - e^{-k_1 t}\right) \quad (3)$$

While the equation corresponding to the pseudo-second-order is expressed as follows:

$$q_t = \frac{k_2 q_e^2 t}{1 + k_2 q_e t} \quad (4)$$

where t is the contact time (min), q_e and q_t are the adsorbed amounts (mg g^{-1}) of COD from PL leachate onto raw bentonite at equilibrium and different times of adsorption, respectively. k_1 (min^{-1}) and k_2 (g mg^{-1} min^{-1}) are the adsorption rate constant related to pseudo-first and pseudo-second-order, respectively.

2.6.3. Isotherm study

The Langmuir and Freundlich models have been used for the experimental adsorption data modeling. In fact, these adsorption isotherms allow designing the leachate adsorption system onto raw bentonite by investigating the adsorbent surface properties and describing the adsorbent–adsorbate affinity [29,38].

Langmuir isotherm model is expressed by the following equation [39]:

$$q_e = \frac{q_m K_L C_e}{1 + K_L C_e} \quad (5)$$

where q_e (mg g^{-1}) is the adsorbed amount at equilibrium, C_e is the equilibrium leachate COD (mg L^{-1}), K_L (L mg^{-1}) is the Langmuir constant related to the energy of adsorption, and q_{max} (mg g^{-1}) is the maximum adsorption capacity.

While Freundlich model is represented by the following expression [40]:

$$q_e = K_F C_e^{1/n} \quad (6)$$

where K_F is Freundlich constant related to the adsorption capacity and n is the heterogeneity factor related to adsorption intensity.

3. Results and discussion

3.1. Bentonite characterization

3.1.1. N_2 gas adsorption–desorption analysis

The adsorption efficiency is highly related to the specific surface area and the porosity of the adsorbent. Thereafter, the N_2 low-temperature adsorption–desorption isotherm was applied using the BET equation [41] to determine the specific surface area (S_{BET} = 51.7 m^2 g^{-1}), the average pore diameter (82.7 Å), and the total pore volume of the bentonite (0.11 cm^3 g^{-1}).

Moreover, Fig. 2 illustrates the N_2 adsorption–desorption isotherm of bentonite adsorbent. The bentonite sample shows a type IV isotherm which presents a remarkable hysteresis loop of H4 at (P/P_0 > 0.4) associated with capillary condensation indicating that the raw bentonite is characterized by a mesoporous structure [42,43]. The mesopores are predominant in the bentonite as indicated by the pore size distribution.

3.1.2. XRD analysis

The XRD patterns provided by Fig. 3 indicates the presence of some characteristic peaks of montmorillonite, as the major mineral of bentonite (2θ = 5.76°, 19.84°, 31.37°, 34.96°, and 62.05°). Additionally, the diffractogram identifies the peaks attributed to calcite at 2θ = 27.73° and quartz at 2θ = 28.53 and 20.63° [24,30,44,45].

3.1.3. SEM-EDX analysis

SEM images (Fig. 4) show the morphology and the microstructure of the granular surface of the natural

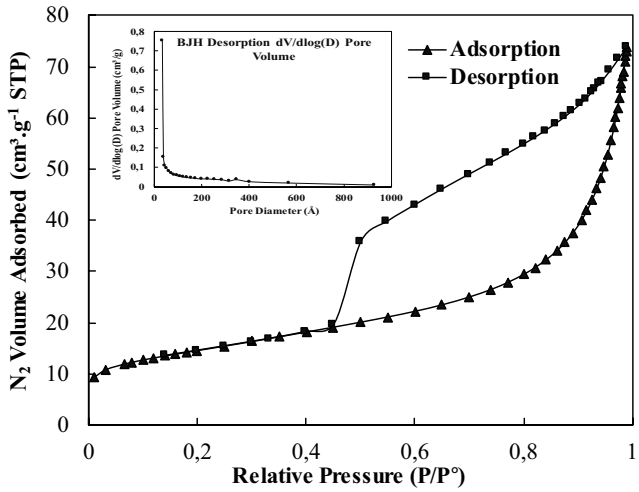

Fig. 2. N_2 adsorption–desorption isotherm and the pore size distribution (inserted figure) of raw bentonite.

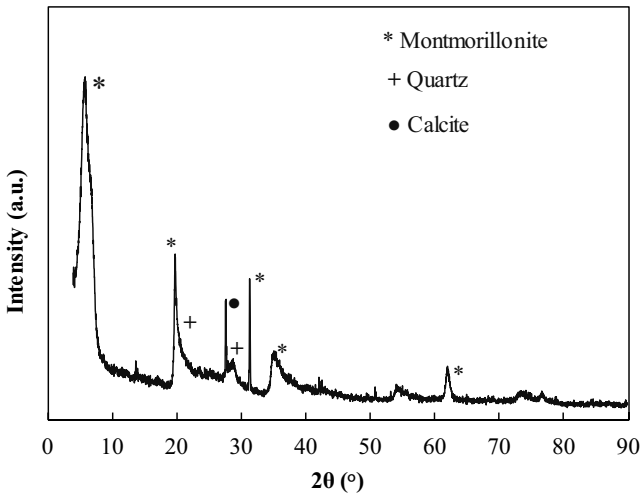

Fig. 3. XRD pattern of raw bentonite.

bentonite. The image (Fig. 4a) reveals a rough surface with heterogeneous particles' structure, while many pores with irregular sizes appear in the image (Fig. 4b).

Fig. 5 illustrates the elementary chemical composition of the raw bentonite obtained by EDX microanalysis. The EDX spectrum indicates that the Moroccan bentonite consists mainly of the elements Si, O, and Al. The attached table presents the percent by weight of the bentonite constituents confirming that Si, O, and Al are the major elements, which are the same for the montmorillonite phase previously determined with XRD. Similar results were obtained by Khatamian et al. [23]. In addition, some elements as C, Fe, Mg, Na, Ca, Cl, K, and Ti, are present with a low percentage.

3.1.4. FTIR analysis of the bentonite

The infrared spectra of raw bentonite (Fig. 6a) showed the presence of Al–O–Si deformation at 520, 692, and 795 cm^{-1} and Si–O stretching at 440 and 611 cm^{-1}. The bands corresponding to Al–Al–OH deformation is noticed at 912 cm^{-1} [25,42,46]. The band with the high intensity appears at 980 cm^{-1} and reveals Si–O stretching vibration [47]. The band 1,110 cm^{-1} is attributed to montmorillonite and 1,637 cm^{-1} corresponds to O–H bend for adsorbed H_2O at bentonite interlayer. The stretching vibration of structural –OH groups is observed at 3,402 cm^{-1}. Moreover, the peak observed at 3,623 cm^{-1} was attributed to a fundamental stretching vibration of different –OH groups present in Al–OH–Al.

In order to investigate the characteristic bands of bentonite after adsorption, Fig. 6b plots the FTIR spectra of bentonite saturated with PL. Where the majority of bands are similar in both spectra. However, new bands with different intensities appeared at 1,444; 3,040; and 2,848 cm^{-1} which could be assigned to a bending vibration of the methylene groups, C–H stretch, and stretching vibrations of $–CH_2$, respectively [29,42]. This remarkable modification of FTIR spectra bands after adsorption could explain the interaction between organic compounds containing in PL and bentonite surface active sites.

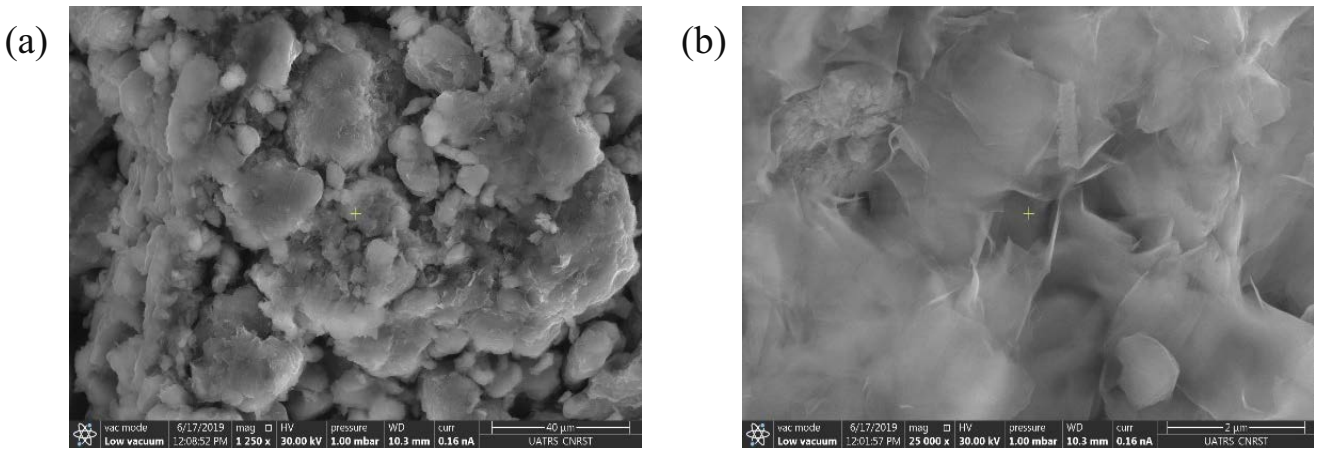

Fig. 4. SEM images of raw bentonite (a) (×1,250) and (b) (×25,000).

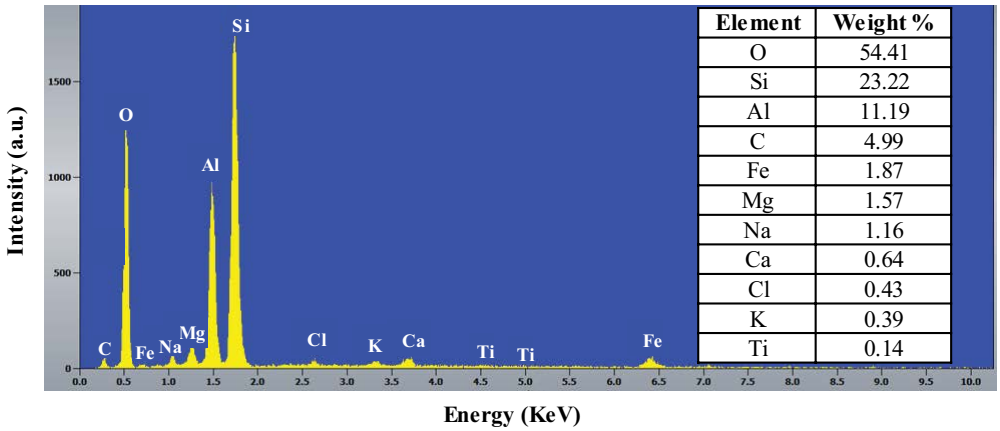

Element	Weight %
O	54.41
Si	23.22
Al	11.19
C	4.99
Fe	1.87
Mg	1.57
Na	1.16
Ca	0.64
Cl	0.43
K	0.39
Ti	0.14

Fig. 5. EDX spectrum of raw bentonite and elementary composition (weight %) of raw bentonite.

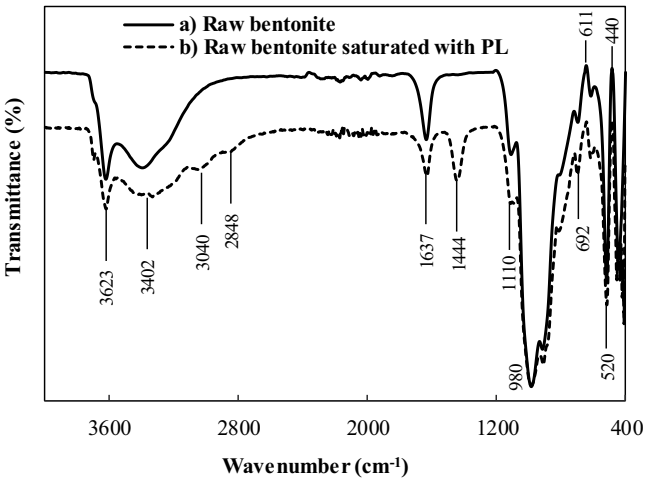

Fig. 6. FTIR spectra of (a) raw bentonite and (b) raw bentonite after PL adsorption.

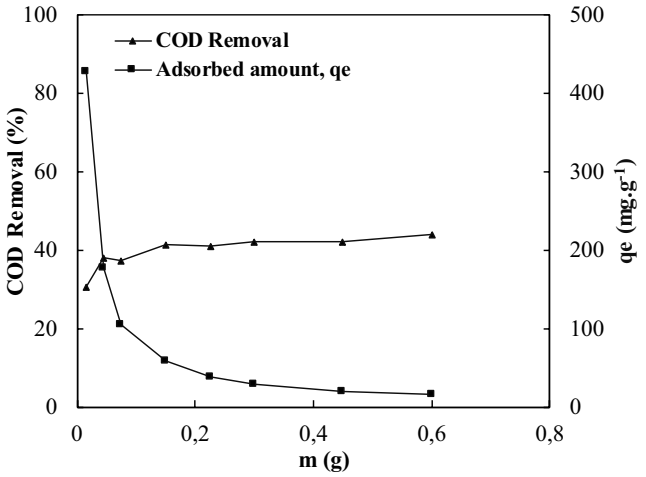

Fig. 7. Effect of bentonite mass on COD removal and adsorbed amount (V = 15 mL; COD_i = 1,400 mg L^{-1}; pH_i = 7; T = 25°C; contact time = 24 h).

3.2. Adsorption of pretreated leachate on raw bentonite

3.2.1. Effect of adsorbent dosage

The adsorbent dosage was initially optimized in terms of COD removal and adsorbed amount of organic compounds of leachate (q_e) as shown in Fig. 7. It is noticed that increasing the mass of raw bentonite from 0.015 to 0.045 g enhanced the COD removal from 30% to 38%. Afterwards, above this mass, the COD removal varied slightly to reach 45% for 0.6 g. Indeed, with more adsorbent amount the surface contact becomes more important leading then to the high availability of active sites, which could explain the evolution of the corresponding results [48]. Hence, the optimal mass of the bentonite was fixed at 3 g L^{-1} of the PL with a COD removal of 38% and an adsorbed amount of 178 mg g^{-1}. This dosage will be used for the next adsorption tests.

3.2.2. Effect of leachate initial pH

Fig. 8 presents the evolution of COD removal and adsorbed amount according to the initial pH values. Indeed, varying the pH values from 3 to 11 has slightly affected the COD removal, where its minimal value 35% was noticed at pH 3, 9, and 11. Though, its maximum 39% was reached at pH = 7 with the highest adsorbed amount of 185 mg g^{-1}. A similar trend was noticed by Li et al. [28] for the removal of bisphenol A from landfill leachate using raw bentonite. However, the high adsorption capacity of bentonite varies from acid to basic pH range, depending on the nature and the complex composition of the aqueous solution [26,31,49,50].

Thus, at acidic pH values, H^+ ions could adhere to active sites of bentonite surface which reduces the accessibility of PL compounds to these sites [51]. While at basic pH, the electrostatic repulsion could become stronger than the binding affinity between the PL and bentonite active sites, because of the high amount of OH^- that could make the charge of PL more negative [26,28,51].

3.2.3. Adsorption kinetic

Fig. 9 illustrates the kinetic of COD adsorption from PL onto bentonite. Hence, the corresponding curve indicates

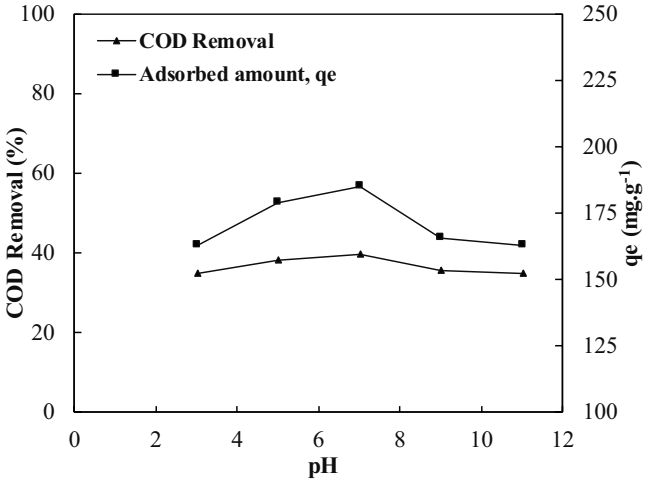

Fig. 8. COD removal and adsorbed amount according to initial pH of PL (V = 15 mL; COD_i = 1,400 mg L^{-1}; m = 0.45 g of bentonite; T = 25°C; contact time = 24 h).

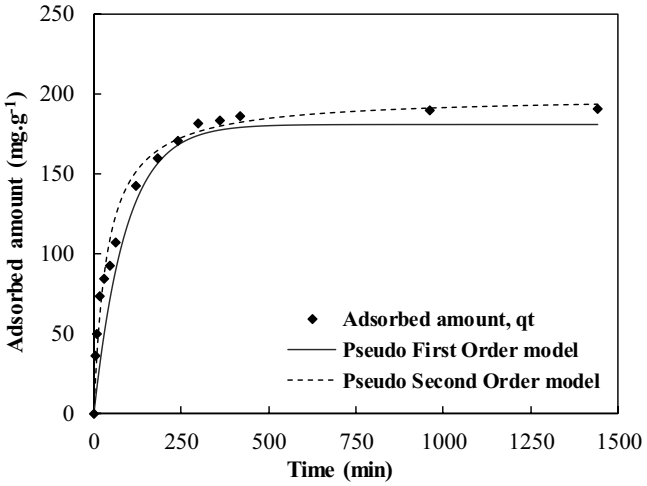

Fig. 9. Kinetic of COD adsorption onto raw bentonite (COD_i = 1,400 mg L^{-1}; m = 3 g of bentonite L^{-1} of PL; pH = 7; T = 25°C).

that the COD amount increased simultaneously with increasing contact time and the adsorption gradually slowed until it reached the equilibrium after 300 min.

In addition, the fitting of kinetic data to the pseudo-first and pseudo-second-order models was illustrated. The parameters' values related to both models are summarized in Table 1.

The results indicate that the pseudo-second-order model is in high agreement with experimental results (R^2 = 0.91) than pseudo-first-order (R^2 = 0.82). This suggests that chemisorption could be the most dominant mechanism which involves the valence forces through electrons sharing and ions exchange between the adsorptive sites of bentonite and PL compounds [52,53].

3.2.4. Adsorption isotherms

Fig. 10 illustrates the adsorbed amount of COD at equilibrium (q_e) vs. the equilibrium COD (C_e) at three temperatures of 25°C, 30°C, and 35°C and their fitting with non-linear models of Langmuir and Freundlich.

The obtained parameters of both models are summarized in Table 2. Hence, the calculated R^2 values for both models were significant (>0.9), while the regression coefficient related to the Freundlich model was the highest for the three temperature levels, which therefore means that is the model the most fitted with the adsorption data of COD on the bentonite, and consequently suggests that the heterogeneous surface and the varied affinity consisting of actives sites with different adsorption potentials [54,55]. Moreover, the maximum adsorption capacities obtained by the Langmuir model were 157, 182, and 195 mg g^{-1} at 25°C, 30°C, and 35°C, respectively, indicating that the endothermic process is dominant [29,56]. This evolution could be due to the fact that increasing the temperature promotes the ions exchange process and the molecules diffusion across the external layer and the internal pores of the adsorbent which enhances the adsorption capacity of raw bentonite [32,57]. In addition, the

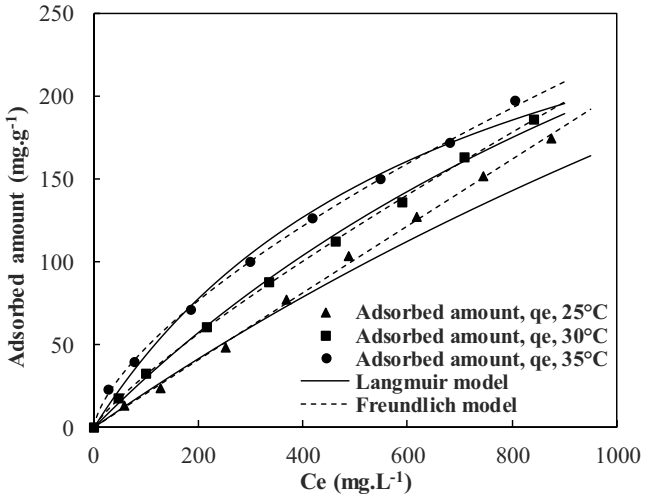

Fig. 10. Equilibrium data of adsorption isotherms and non-linear models of Langmuir and Freundlich, at 25°C, 30°C, and 35°C (m = 3 g of bentonite L^{-1} of PL; pH = 7; contact time = 5 h).

bentonite as one of the montmorillonite clays is characterized by a lattice of positive thermal expansion coefficient which improves the adsorbate mobility onto the surface layer of the adsorbent by rising the temperature [57,58].

3.3. UV-visible spectra evolution of raw leachate, PL, and PL adsorbed onto bentonite

The UV-visible spectrum of leachate is an important indicator of sample composition in terms of organic matter. Indeed, the absorbance values are highly proportional to the amount and complexity of organic compounds [59]. Essentially, the range of 200–400 nm indicates the presence of polycyclic aromatic compounds, and macromolecules with carbonyl and conjugated double bonds, such as hydrocarbons, fulvic, and humic acids [60–62].

Table 1
Kinetic parameters of pseudo-first and pseudo-second-order models of PL adsorption onto bentonite

Pseudo-first-order model				Pseudo-second-order model			
q_{exp}	q_e	k_1	R^2	q_{exp}	q_e	k_2	R^2
181	178	0.011	0.82	181	191	0.00014	0.91

Table 2
Langmuir and Freundlich parameters of COD adsorption onto bentonite

	Langmuir model			Freundlich model		
	q_{max}	K_L	R^2	K_F	n	R^2
25°C	157	0.0014	0.9755	0.2128	1.0074	0.9964
30°C	182	0.0018	0.9863	0.7082	1.2089	0.9976
35°C	191	0.0026	0.9845	2.2659	1.5029	0.9982

In order to provide further information about the treatment efficiency, Fig. 11 plots the UV-visible spectra before and after both processes treatment (Fenton and adsorption). Where, the spectrum of raw leachate is characterized with high absorbance values, therefore confirming its high pollutant load previously indicated by COD value [61]. Thereafter, a significant decrease in the UV-visible spectrum is noticed after the pretreatment (PL), indicating that the majority of organic pollutants have been degraded during the Fenton process [60,62]. Moreover, a further decrease is noticed for the absorbance values related to PL adsorbed onto bentonite, especially in the wavelength range 250–300 nm. Which explains the removal of organic compounds by the porous surface of raw bentonite, and confirms the trend of COD removal in the previous figures of adsorption tests [4,61,63]. In addition, this spectra evolution correlates with the coloration difference of three leachate samples presented by the attached image,

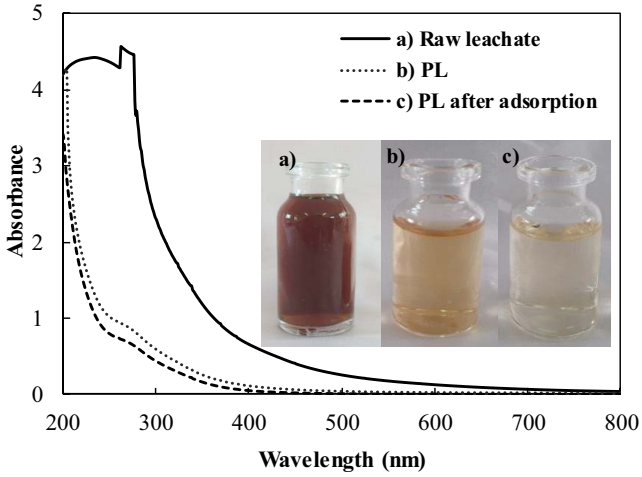

Fig. 11. UV-visible spectra corresponding to: (a) raw leachate, (b) PL, and (c) PL adsorbed onto bentonite.

where a significant discoloration is noticed for PL and PL adsorbed onto bentonite, compared with dark raw leachate.

3.4. Treatment efficiency

Table 3 summarizes the main physical-chemical characteristics of landfill leachate before and after treatment using the Fenton process alone or the combination of the Fenton and the adsorption process. The results show a significant decrease in the values of all parameters (turbidity, color number, COD, BOD_5, chlorides, N-nitrates, N-nitrites, phosphates, N-ammonium, Cr, Cu, and Mn) after Fenton treatment. Thereafter, using the natural bentonite for the adsorption process enhanced the pollutants' removal where a further decrease was noticed in all leachate characteristics. Consequently, the combination of both processes was effectively applied for the treatment of landfill leachate and could be successfully suggested as a promising technology for hazardous effluents.

Table 3
Main physical–chemical parameters for raw and treated leachate

Parameters	Raw leachate	Fenton	Combined Fenton and adsorption	Cumulative removal (%)
Turbidity, NTU	250	10	8	97
Color number	6.48	0.223	0.143	98
COD, mg L^{-1}	5,198	1,400	832	84
BOD_5, mg L^{-1}	500	210	25	95
Chlorides, mg L^{-1}	5,230	1,048	511	90
N-nitrates, mg L^{-1}	6.43	0.172	0.73	88
N-nitrites, mg L^{-1}	5.98	0.45	1.95	67
Phosphates, mg L^{-1}	0.32	0.0023	0.001	99.7
N-ammonium, mg L^{-1}	831	327	125	85
Cr, mg L^{-1}	1.65	<0.01	<0.01	100
Cu, mg L^{-1}	0.1	0.02	<0.01	100
Mn, mg L^{-1}	0.04	<0.01	<0.01	100

Table 4
Comparison of adsorption process efficiency applied on various leachate samples from different countries

Country	Pretreatment process	Adsorbent	Adsorbate	Total efficiency (%)	Reference
Fez, Morocco	Fenton	Natural bentonite	COD	84	Present study
			Color	98	
Merida, Yucatan, Mexico	Fenton	Commercial AC	Color	99	[64]
			COD	99	
Coquimbo, Chile	Filtration	AC obtained from coffee waste	COD	51	[65]
			Copper	97.1	
Coquimbo, Chile	Coagulation–flocculation	AC obtained from fish scales	COD	37.3	[66]
			Color	60.1	
Penang, Malaysia	Semi-aerobic landfill leachate	Composite AC-Zeolite	COD	86.4	[67]
			NH_3–N	92.6	
Penang, Malaysia	Filtration	Nanoparticles Fe_2O_3	Color	97	[68]
			COD	75.9	
			NH_3–N	43.8	
Perak, Malaysia	NA	AC from sugarcane bagasse	Color	94.74	[6]
			COD	83.61	
			NH_3–N	46.65	
Casablanca, Morocco	Coagulation–flocculation	Commercial AC	COD	77	[4]
			Color	99.7	
Skopje, Macedonia	NA	Natural bentonite	Fe(II)	95.78	[69]
			Zn(II)	98.82	
Qazvin, Iran	NA	Amino acid modified bentonite	COD	65.7	[70]
Penang, Malaysia	Semi-aerobic landfill leachate	AC from tamarind fruit seed	COD	79.93	[71]

AC: Activated carbon; NA: Pretreatment no applicable.

The efficiency of leachate treatment is strongly related to its composition that varies from one country to another and even between cities of the same country, depending on the composition of solid waste, landfilling, and climate.

To compare the results of the present study to other research works, Table 4 presents previous studies reporting the application of the adsorption process on raw leachate or preceded by different treatment processes [4,6,64–71]. The removal values vary substantially from one study to another according to the adsorbent used, the target adsorbate, the applied pretreatment process, and the leachate quality. Indeed, leachate treatment is strongly related to its composition that varies from one country to another [72,73]. However, the obtained findings from the present study are considered encouraging and promising consistently in line with the eco-efficiency of the applied processes.

Overall, landfill leachate is a highly loaded and complex effluent affected by diverse factors. Hence, it is often difficult to select the most appropriate process, which requires the combination of two or more treatment steps as the most indispensable solution to reduce the refractory organic compounds and reach the strict discharge standards [74,75].

4. Conclusion

This work investigated the application of raw bentonite as a low-cost and available natural adsorbent for the enhancement of pollutants removal from treated leachate with the Fenton process. Indeed, the raw bentonite was firstly characterized, afterwards, the adsorption tests of pretreated leachate in the batch system have been carried out. Where, the effect of adsorbent mass, initial PL pH, contact time, and the temperature was examined.

Hence, applying the adsorption process as a second treatment enhanced the effectiveness of leachate treatment with the elimination of 84% for COD and 98% of color, using 3 g of bentonite L^{-1} at neutral pH and 35°C during 5 h of contact time. The experimental data were well described with pseudo-second-order kinetic model and Freundlich isotherm model. Finally, this study provided an efficient processes combination for removing the majority of pollutants from the stabilized leachate of Fez city (Morocco), and which could be effectively used for other liquid effluents depollution.

References

[1] H.S. Erkan, O. Apaydin, Final treatment of young, middle-aged, and stabilized leachates by Fenton process: optimization by response surface methodology, Desal. Water Treat., 54 (2015) 342–357.
[2] A. Sil, S. Kumar, Chapter 17 – Landfill Leachate Treatment, J.W.-C. Wong, R.D. Tyagi, A. Pandey, Current Developments in Biotechnology and Bioengineering, 1st ed., Solid Waste Management, Elsevier B.V., Amsterdam, 2017, pp. 391–406.
[3] H. Ehrig, R. Stegmann, Chapter 10.5 – Combination of Different MSW Leachate Treatment Processes, R. Cossu, R. Stegmann,

Eds., Solid Waste Landfilling Concepts, Processes Technology, Elsevier Inc., Amsterdam, 2019, pp. 633–646.
[4] Z. Chaouki, F. Khalil, M. Ijjaali, H. Valdés, S. Rafqah, M. Sarakha, H. Zaitan, Use of combination of coagulation and adsorption process for the landfill leachate treatment from Casablanca city, Desal. Water Treat., 83 (2017) 262–271.
[5] I. El Mrabet, M. Benzina, H. Valdés, H. Zaitan, Treatment of landfill leachates from Fez city (Morocco) using a sequence of aerobic and fenton processes, Sci. Afr., 8 (2020), doi: 10.1016/j.sciaf.2020.e00434.
[6] N.B. Azmi, M.J.K. Bashir, S. Sethupathi, C.A. Ng, Anaerobic stabilized landfill leachate treatment using chemically activated sugarcane bagasse activated carbon: kinetic and equilibrium study, Desal. Water Treat., 57 (2014) 3916–3927.
[7] M. Assou, L. El Fels, A. El Asli, H. Fakidi, S. Souabi, M. Hafidi, Landfill leachate treatment by a coagulation–flocculation process : effect of the introduction order of the reagents, Desal. Water Treat., 57 (2016) 21817–21826.
[8] M. Hassan, X. Wang, F. Wang, D. Wu, A. Hussain, B. Xie, Coupling ARB-based biological and photochemical (UV/TiO_2 and UV/$S_2O_8^{2-}$) techniques to deal with sanitary landfill leachate, Waste Manage., 63 (2017) 292–298.
[9] R. Li, B. Wang, O. Owete, J. Dertien, C. Lin, H. Ahmad, G. Chen, Landfill leachate treatment by electrocoagulation and fiber filtration, Water Environ. Res., 89 (2017) 2015–2020.
[10] I. El Mrabet, M. Benzina, H. Zaitan, Optimization of persulfate/iron(II)/UV-A irradiation process for the treatment of landfill leachate from Fez City (Morocco), SN Appl. Sci., 2 (2020), doi: 10.1007/s42452-020-2868-z.
[11] Y. Cherni, L. Elleuch, M. Messaoud, K. Djebali, M. Kasmi, R. Salhi, A. Chatti, I. Trabelsi, New trend of Jebel Chakir landfill leachate pre-treatment by photocatalytic TiO_2/Ag nanocomposite prior to fermentation using *Candida tropicalis* strain, Int. Biodeterior. Biodegrad., 146 (2020) 104829 1–10, doi: 10.1016/j.ibiod.2019.104829.
[12] A. Amiri, M.R. Sabour, Multi-response optimization of Fenton process for applicability assessment in landfill leachate treatment, Waste Manage., 34 (2014) 2528–2536.
[13] F. Mahdad, H. Younesi, N. Bahramifar, M. Hadavifar, Optimization of Fenton and photo-Fenton-based advanced oxidation processes for post-treatment of composting leachate of municipal solid waste by an activated sludge process, KSCE J. Civ. Eng., 20 (2015) 2177–2188.
[14] Y. Chen, C. Liu, J. Nie, S. Wu, D. Wang, Removal of COD and decolorizing from landfill leachate by Fenton's reagent advanced oxidation, Clean Technol. Environ. Policy, 16 (2014) 189–193.
[15] D. Trujillo, X. Font, A. Sánchez, Use of Fenton reaction for the treatment of leachate from composting of different wastes, J. Hazard. Mater., 138 (2006) 201–204.
[16] A. Žgajnar Gotvajn, J. Zagorc-Koncan, M. Cotman, Fenton's oxidative treatment of municipal landfill leachate as an alternative to biological process, Desalination, 275 (2011) 269–275.
[17] S.K. Singh, W.Z. Tang, G. Tachiev, Fenton treatment of landfill leachate under different COD loading factors, Waste Manage., 33 (2013) 2116–2122.
[18] M. Hadri, Z. Chaouki, K. Draoui, M. Nawdali, A. Barhoun, H. Valdés, N. Drouiche, H. Zaitan, Adsorption of a cationic dye from aqueous solution using low-cost moroccan diatomite: adsorption equilibrium, kinetic and thermodynamic studies, Desal. Water Treat., 75 (2017) 213–224.
[19] Z. Bencheqroun, I. El Mrabet, M. Kachabi, M. Nawdali, H. Valdés, I. Neves, H. Zaitan, Removal of basic and acid dyes from aqueous solutions using cone powder from Moroccan Cypress Cupressus sempervirens as a natural adsorbent, Desal. Water Treat., 166 (2019) 387–398.
[20] A. Dra, K. Tanji, A. Arrahli, E.M. Iboustaten, A. El Gaidoumi, A. Kherchafi, A.C. Benabdallah, A. Kherbeche, Valorization of Oued Sebou natural sediments (Fez-Morocco area) as adsorbent of methylene blue dye: kinetic and thermodynamic study, Sci. World J., 2020 (2020), doi: 10.1155/2020/4815767.
[21] M. Gaouar Yadi, B. Benguella, N. Gaouar-Benyelles, K. Tizaoui, Adsorption of ammonia from wastewater using low-cost bentonite/chitosan beads, Desal. Water Treat., 57 (2016) 21444–21454.
[22] M.E. Mahmoud, A.M. El-ghanam, R.H.A. Mohamed, S.R. Saad, Enhanced adsorption of levofloxacin and ceftriaxone antibiotics from water by assembled composite of nanotitanium oxide/chitosan/nano-bentonite, Mater. Sci. Eng., C, 108 (2020) 110199 1–14, doi: 10.1016/j.msec.2019.110199.
[23] M. Khatamian, B. Divband, R. Shahi, Ultrasound assisted co-precipitation synthesis of Fe_3O_4/bentonite nanocomposite: performance for nitrate, BOD and COD water treatment, J. Water Process Eng., 31 (2019) 100870 1–12, doi: 10.1016/j.jwpe.2019.100870.
[24] A. Oussalah, A. Boukerroui, A. Aichour, B. Djellouli, Cationic and anionic dyes removal by low-cost hybrid alginate/natural bentonite composite beads: adsorption and reusability studies, Int. J. Biol. Macromol., 124 (2019) 854–862.
[25] D. Borschneck, S. Bel-Abbes, Urban wastewater treatment by adsorption of organic matters on modified bentonite by (iron-aluminum), J. Encapsulation Adsorpt. Sci., 4 (2014) 71–79.
[26] E. Derakhshani, A. Naghizadeh, Optimization of humic acid removal by adsorption onto bentonite and montmorillonite nanoparticles, J. Mol. Liq., 259 (2018) 76–81.
[27] S.M. Raghab, A.M. Abd El Meguid, H.A. Hegazi, Treatment of leachate from municipal solid waste landfill, HBRC J., 9 (2013) 187–192.
[28] Y. Li, F. Jin, C. Wang, Y. Chen, Q. Wang, W. Zhang, D. Wang, Modification of bentonite with cationic surfactant for the enhanced retention of bisphenol A from landfill leachate, Environ. Sci. Pollut. Res., 22 (2015) 8618–8628.
[29] M. Bergaoui, A. Nakhli, Y. Benguerba, M. Khalfaoui, A. Erto, F. Edi, S. Ismadji, B. Ernst, Novel insights into the adsorption mechanism of methylene blue onto organo-bentonite: adsorption isotherms modeling and molecular simulation, J. Mol. Liq., 272 (2018) 697–707.
[30] M. Hajjaji, H. El Arfaoui, Adsorption of methylene blue and zinc ions on raw and acid-activated bentonite from Morocco, Appl. Clay Sci., 46 (2009) 418–421.
[31] Z. Huang, Y. Li, W. Chen, J. Shi, N. Zhang, X. Wang, Z. Li, L. Gao, Y. Zhang, Modified bentonite adsorption of organic pollutants of dye wastewater, Mater. Chem. Phys., 202 (2017) 266–276.
[32] J.G. Meneguin, M.P. Moisés, T. Karchiyappan, S.H.B. Faria, M.L. Gimenes, M.A.S.D. de Barros, S. Venkatachalam, Preparation and characterization of calcium treated bentonite clay and its application for the removal of lead and cadmium ions: adsorption and thermodynamic modeling, Process Saf. Environ. Prot., 111 (2017) 244–252.
[33] I. El Mrabet, M. Kachabi, M. Nawdali, A. Harrach, F. Khalil, M. Ijjaali, M. Benzina, H. Zaitan, Treatment of landfill leachate from Fez city (Morocco) using Fenton and photo-Fenton processes, IOP Conf. Ser.: Earth Environ. Sci., 161 (2018) 012025 1–9, doi: 10.1088/1755-1315/161/1/012025.
[34] J. Rodier, B. Legube, N. Merlet, L'Analyse de L'eau, 9th ed., Dunod, Paris, 2009.
[35] J. Li, T. Tao, X. Bin Li, J. Lan Zuo, T. Li, J. Lu, S. Hui Li, L. Zhen Chen, C. Yang Xia, Y. Liu, Y. Li Wang, A spectrophotometric method for determination of chemical oxygen demand using home-made reagents, Desalination, 239 (2009) 139–145.
[36] G. Fagerlund, Determination of specific surface by the BET method, Matériaux Constr., 6 (1973) 239–245.
[37] S. Lagergren, About the theories of so-called adsorption of soluble substance, Sven. Vetenskapsakad. Handingarl. Band, 24 (1898) 1–39.
[38] K. Elass, A. Laachach, A. Alaoui, M. Azzi, Removal of methyl violet from aqueous solution using a stevensite-rich clay from Morocco, Appl. Clay Sci., 54 (2011) 90–96.
[39] I. Langmuir, The constitution and fundamental properties of solids and liquids. Part I. Solids, J. Am. Chem. Soc., 38 (1916) 2221–2295.
[40] H. Freundlich, W. Heller, The adsorption of cis- and trans-azobenzene, J. Am. Chem. Soc., 61 (1939) 2228–2230.
[41] S. Brunauer, P.H. Emmett, E. Teller, Adsorption of gases in multimolecular layers, J. Am. Chem. Soc., 60 (1938) 309–319.

[42] A. Kurniawan, H. Sutiono, Y. Ju, F. Edy, A. Ayucitra, A. Yudha, S. Ismadji, Utilization of rarasaponin natural surfactant for organo-bentonite preparation: application for methylene blue removal from aqueous effluent, Microporous Mesoporous Mater., 142 (2011) 184–193.
[43] Z. Bencheqroun, Z. Chaouki, M. Hadri, M. Nawdali, K. Draoui, H. Valdés, H. Zaitan, Removal of textile dyes from aqueous solutions using low cost Moroccan clay, IOP Conf. Ser.: Earth Environ. Sci., 161 (2018) 012009 1–10, doi: 10.1088/1755-1315/161/1/012009.
[44] O. Assila, K. Tanji, M. Zouheir, A. Arrahli, L. Nahali, F. Zerrouq, A. Kherbeche, Adsorption studies on the removal of textile effluent over two natural eco-friendly adsorbents, J. Chem., 2020 (2020) 1–13.
[45] A. Bouazizi, S. Saja, B. Achiou, M. Ouammou, J.I. Calvo, A. Aaddane, S.A. Younssi, Elaboration and characterization of a new flat ceramic MF membrane made from natural Moroccan bentonite. Application to treatment of industrial wastewater, Appl. Clay Sci., 132–133 (2016) 33–40.
[46] A. Dra, A. El Gaidoumi, K. Tanji, A. Chaouni Benabdallah, A. Taleb, A. Kherbeche, Characterization and quantification of heavy metals in Oued Sebou sediments, Sci. World J., 2019 (2019) 21–23.
[47] A. Manni, A. Elhaddar, A. El Bouari, I.E. El Amrani El Hassani, C. Sadik, Complete characterization of Berrechid clays (Morocco) and manufacturing of new ceramic using minimal amounts of feldspars: economic implication, Case Stud. Constr. Mater., 7 (2017) 144–153.
[48] A.B. Karim, B. Mounir, M. Hachkar, M. Bakasse, A. Yaacoubi, Removal of Basic Red 46 dye from aqueous solution by adsorption onto Moroccan clay, J. Hazard. Mater., 168 (2009) 304–309.
[49] H. Cheng, Q. Zhu, Z. Xing, Adsorption of ammonia nitrogen in low temperature domestic wastewater by modification bentonite, J. Cleaner Prod., 233 (2019) 720–730.
[50] Syafalni, R. Abdullah, I. Abustan, A.N.M. Ibrahim, Wastewater treatment using bentonite, the combinations of bentonite-zeolite, bentonite-alum, and bentonite-limestone as adsorbent and coagulant, Int. J. Environ. Sci., 4 (2013) 379–391.
[51] D. Sivakumar, Adsorption study on municipal solid waste leachate using *Moringa oleifera* seed, Int. J. Environ. Sci. Technol., 10 (2013) 113–124.
[52] Q. Liu, P. Hu, J. Wang, L. Zhang, R. Huang, Phosphate adsorption from aqueous solutions by Zirconium(IV) loaded cross-linked chitosan particles, J. Taiwan Inst. Chem. Eng., 59 (2016) 311–319.
[53] Y. Zhou, Y. He, Y. Xiang, S. Meng, X. Liu, J. Yu, J. Yang, J. Zhang, P. Qin, L. Luo, Single and simultaneous adsorption of pefloxacin and Cu(II) ions from aqueous solutions by oxidized multiwalled carbon nanotube, Sci. Total Environ., 646 (2019) 29–36.
[54] A.S. Hamid, M. Shahadat, S. Ismail, Development of cost effective bentonite adsorbent coating for the removal of organic pollutant, Appl. Clay Sci., 149 (2017) 79–86.
[55] I. Anastopoulos, G.Z. Kyzas, Are the thermodynamic parameters correctly estimated in liquid-phase adsorption phenomena?, J. Mol. Liq., 218 (2016) 174–185.
[56] J. Wang, Z. Chen, D. Shao, Y. Li, Z. Xu, C. Cheng, A.M. Asiri, H.M. Marwani, S. Hu, Adsorption of U(VI) on bentonite in simulation environmental conditions, J. Mol. Liq., 242 (2017) 678–684.
[57] C.A.P. Almeida, N.A. Debacher, A.J. Downs, L. Cottet, C.A.D. Mello, Removal of methylene blue from colored effluents by adsorption on montmorillonite clay, J. Colloid Interface Sci., 332 (2009) 46–53.
[58] A.S. Özcan, B. Erdem, A. Özcan, Adsorption of Acid Blue 193 from aqueous solutions onto Na-bentonite and DTMA-bentonite, J. Colloid Interface Sci., 280 (2004) 44–54.
[59] Z. Liu, X. Li, Z. Rao, F. Hu, Treatment of landfill leachate biochemical effluent using the nano-Fe_3O_4/$Na_2S_2O_8$ system: oxidation performance, wastewater spectral analysis, and activator characterization, J. Environ. Manage., 208 (2018) 159–168.
[60] Z. Liu, W. Wu, P. Shi, J. Guo, J. Cheng, Characterization of dissolved organic matter in landfill leachate during the combined treatment process of air stripping, Fenton, SBR and coagulation, Waste Manage., 41 (2015) 111–118.
[61] O. Thomas, G. Junqua, M.-F. Thomas, Chapter 11 – Leachates and Organic Extracts From Solids, O. Thomas, C. Burgess, Eds., UV-Visible Spectrophotometry Water Wastewater, 2nd ed., Elsevier, Amsterdam, 2017, pp. 349–378.
[62] E. Touraud, J. Roussy, M. Domeizel, G. Junqua, O. Thomas, Chapter 10 – Leachates and Organic Extracts From Solids, O. Thomas, C. Burgess, Eds., Techniques and Instrumentation in Analytical Chemistry, Elsevier BV, Amsterdam, 2007, pp. 243–265.
[63] O. Thomas, F. Theraulaz, S. Vaillant, M.-F. Pouet, Chapter 8 – Urban Wastewater, O. Thomas, C. Burgess, Eds., UV-Visible Spectrophotometry of Water and Wastewater. Techniques and Instrumentation in Analytical Chemistry, Elsevier, Amsterdam, 2007, pp. 189–216.
[64] L. San-Pedro, R. Méndez-Novelo, E. Hernández-Núñez, M. Flota-Bañuelos, J. Medina, G. Giacomán-Vallejos, Selection of the activated carbon type for the treatment of landfill leachate by Fenton-adsorption process, Molecules, 25 (2020) 3023 1–16, doi: 10.3390/molecules25133023.
[65] Chávez, Y.L. Galiano, Landfill leachate treatment using activated carbon obtained from coffee waste, Eng. Sanit. Ambient., 24 (2019) 833–842.
[66] R. Poblete, E. Cortes, J. Bakit, Y. Luna-Galiano, Use of fish scales as an adsorbent of organic matter present in the treatment of landfill leachate, J. Chem. Technol. Biotechnol., 95 (2020) 1550–1558.
[67] A.A. Halim, H.A. Aziz, M.A.M. Johari, K.S. Ariffin, M.N. Adlan, Ammoniacal nitrogen and COD removal from semi-aerobic landfill leachate using a composite adsorbent: fixed bed column adsorption performance, J. Hazard. Mater., 175 (2010) 960–964.
[68] A.M.H. Shadi, M.A. Kamaruddin, N.M. Niza, M.I. Emmanuel, M.S. Hossain, N. Ismail, Efficient treatment of raw leachate using magnetic ore iron oxide nanoparticles Fe_2O_3 as nanoadsorbents, J. Water Process Eng., 38 (2020) 101637 1–9, doi: 10.1016/j.jwpe.2020.101637.
[69] K. Atkovska, B. Bliznakovska, G. Ruseska, S. Bogoevski, B. Boskovski, A. Grozdanov, Adsorption of Fe(II) and Zn(II) ions from landfill leachate by natural bentonite, J. Chem. Technol. Metall., 51 (2016) 215–222.
[70] M. Hajjizadeh, S. Ghammamy, H. Ganjidoust, F. Farsad, Amino acid modified bentonite clay as an eco-friendly adsorbent for landfill leachate treatment, Pol. J. Environ. Stud., 29 (2019) 4089–4099.
[71] K.Y. Foo, L.K. Lee, B.H. Hameed, Batch adsorption of semi-aerobic landfill leachate by granular activated carbon prepared by microwave heating, Chem. Eng. J., 222 (2013) 259–264.
[72] Z. Youcai, Chapter 1 - Leachate Generation and Characteristics, Z. Youcai, Eds., Pollution Control Technology for Leachate from Municipal Solid Waste, Elsevier BV, Amsterdam, 2018, pp. 1–30.
[73] H. Luo, Y. Zeng, Y. Cheng, D. He, X. Pan, Recent advances in municipal landfill leachate: a review focusing on its characteristics, treatment, and toxicity assessment, Sci. Total Environ., 703 (2020) 135468 1–19, doi: 10.1016/j.scitotenv.2019.135468.
[74] V. Torretta, N. Ferronato, I.A. Katsoyiannis, A.K. Tolkou, M. Airoldi, Novel and conventional technologies for landfill leachates treatment: a review, Sustainability, 9 (2017) 1–39.
[75] B. Fitzke, T. Blume, H. Wienands, Á. Cambiella, Hybrid Processes for the Treatment of Leachate from Landfills, J. Coca-Prados, G. Gutiérrez-Cervelló, Eds., Economic Sustainability and Environmental Protection in Mediterranean Countries through Clean Manufacturing Methods, Springer Science+Business Media, Dordrecht, 2013, pp. 107–126.